Science
AAAS

Supplementary Materials for

Membrane-associated periodic skeleton is a signaling platform for RTK transactivation in neurons

Ruobo Zhou, Boran Han, Chenglong Xia, Xiaowei Zhuang*

* Correspondence to: zhuang@chemistry.harvard.edu

This PDF file includes:

Materials and Methods

Figs. S1 to S19

References 40-48

Materials and Methods

Primary culture of mouse hippocampal neurons

All experimental procedures were performed in accordance with the Guide for the Care and Use of Laboratory Animals of the National Institutes of Health. The protocol was approved by the Institutional Animal Care and Use Committee (IACUC) of Harvard University. Primary cultures of hippocampal neurons were prepared as previously described (*12*). Briefly, timed pregnant CFW mice (Strain code 024, Charles River Laboratories, Wilmington, MA) were euthanized, and hippocampi were isolated from mouse embryos (E18) and digested with 0.25% trypsin-EDTA (1x) (Sigma, T4549) at 37 °C for 15 minutes. The digested tissues were washed with Hanks' Balanced Salt Solution (HBSS) (Thermo Fisher Scientific, 14175079) for three times, and then transferred to culture medium consisting of Neurobasal medium (Thermo Fisher Scientific, 21103049) supplemented with 37.5 mM NaCl, 2% (vol/vol) B27 supplement (Thermo Fisher Scientific, 17504044) and 1% (vol/vol) Glutamax (Thermo Fisher Scientific, 35050-061). The tissues were gently triturated in the culture medium until there was no chunks of tissue left. Dissociated cells were then counted and plated onto poly-D-lysine-coated 18-mm coverslips (NeuVitro, GG-18-1.5-pdl). Neuronal cultures were maintained in the culture medium in a humidified atmosphere of 5% CO_2 at 37 °C. The neurons were fed with one-half medium volume change every five days.

Antibodies

The following primary antibodies were used in this study: guinea pig anti-MAP2 antibody (Synaptic Systems, 188004), rabbit anti-MAP2 antibody (Synaptic Systems, 188002), mouse anti-βII spectrin antibody (BD Biosciences, 612563), rabbit anti-βII spectrin antibody (Novus Biologicals, NB100-40829), mouse anti-pERK antibody (Celling Signaling, 5726S), rabbit anti-phospho-ERK antibody (Celling Signaling, 4370S), rabbit anti-ERK antibody (Celling Signaling, 4695S), rabbit anti-phospho-TrkB antibody (Thermo Fisher Scientific, PA5-38077), rabbit anti-TrkB antibody (Biovision, 3593), rabbit anti-phospho-FGFR antibody (Celling Signaling,52928S), rabbit anti-FGFR1 antibody (Celling Signaling, 9740S), rabbit anti-CB1 antibody (Alomone Labs, ACR-001), mouse anti-CB1 antibody (Santa Cruz, sc-518035), rabbit anti-NCAM1 antibody (EMD Millipore, AB5032), rat anti-NCAM1 antibody (EMD Millipore, MAB310), mouse anti-NCAM1 antibody (Abcam, ab9018), rabbit IgG isotype control (Santa Cruz Biotechnology, sc-2027), chicken anti-GFP antibody (Thermo Fisher Scientific, A10262). rabbit anti-calpain-2 antibody (Proteintech, 11472-1-AP), rabbit anti-β-actin antibody (Proteintech, 20536-1-AP).

The following secondary antibodies were used in this study: CF680-conjugated donkey anti-mouse IgG antibody (Biotium, 20819), CF680-conjugated donkey anti-chicken IgY antibody (Jackson ImmunoResearch, 703-005-155; Antibody was labeled with CF680 NHS ester to achieve a dye labeling ratio of ~1 dye per antibody), Alexa-647-conjugated donkey anti-mouse IgG antibody (Jackson ImmunoResearch, 715-605-151), Alexa-647-conjugated donkey anti-rabbit IgG antibody (Jackson ImmunoResearch, 711-605-152), Alexa-647-conjugated donkey anti-chicken IgY antibody (Jackson ImmunoResearch, 703-605-155), Alexa-647-conjugated donkey anti-goat IgG antibody (Thermo Fisher Scientific, A21447), Alexa-546-conjugated donkey anti-rabbit IgG antibody (Thermo Fisher Scientific, A10040), Cy3-conjugated donkey anti-guinea pig IgG antibody (Jackson ImmunoResearch, 706-165-148), Alexa-488-conjugated donkey rabbit IgG antibody (Jackson ImmunoResearch, 711-545-152). Alexa-488-conjugated donkey anti-guinea pig IgG antibody (Jackson ImmunoResearch, 706-545-148).

Lentivirus production and transduction of hippocampal neurons

Plasmids used in this study were purchased from GeneCopoeia or OriGene, and cloned into lentiviral expression vector FUGW (Addgene, Plasmid #14883), through Gibson assembly reaction (New England Biolabs, E5510S) according to the manufacturer's protocol. Specifically, *Fgfr1* (Gene Script, OMu23155D), *Fyn* (GeneCopoeia, EX-Mm28528-M98), *Ntrk2* (Addgene, Plasmid #83952), *Src* (GeneCopoeia, EX-Mm05452-M98), Src^{Act} (Src with mutations K257E, P258E and Y535F), Src^{SH2eng} (Src with mutations Q536E, P537E and G538I), $Src^{SH2\text{-}3eng}$ (Src with mutations K257P, T260P, Q261P, Q536E, P537E and G538I) were tagged at their C terminus with the *Gfp* gene through a sequence encoding a flexible polypeptide linker and cloned into FUGW vector. Src contains four intramolecular domains, including the N-terminal SH4 domain containing the lipidation site for membrane localization, the SH3 and SH2 domains that can potentially interact with and recruit the kinase substrates, and the C-terminal SH1 kinase domain. The three GFP-tagged Src mutants were based on a previous study to bias the Src activity toward different kinase activation states (*31*): 1) Src^{Act}, a constitutively active mutant containing mutations that disrupt the interactions between the SH2-SH1 linker and the SH3 domain as well as between the C-terminal tail and the SH2 domain; 2) Src^{SH2eng}, a SH2 domain-engaged mutant containing a high affinity sequence in the Src C-terminal tail for SH2 binding to inhibit Src kinase activity and substrate interactions with SH2; 3) $Src^{SH2\text{-}3eng}$, a SH2- and SH3-engaged mutant containing all mutations for $Src^{SH2eng\ and}$ as well as a high affinity sequence in the SH2-SH1 linker for SH3 binding, to inhibit Src kinase activity and substrate interactions with SH2 and SH3. All the constructs were verified by DNA sequencing.

Lentiviruses were then produced by co-transfecting Lenti-X 293 cells with 6 μg lentiviral expression vector expressing the molecule of interest, 4.5 μg Δ8.9 vector (*40*) (gift from Prof. David Baltimore, California Institute of Technology) and 3 μg VSVG packaging vector (Addgene, Plasmid #8454) in a 10 cm petri dish using FuGENE HD Transfection Reagent (Promega, E2311). Two days post-transfection, the supernatant was harvested, centrifuged at 3000 rpm for 10 min, and then concentrated with Lenti-X concentrator (Clontech, 631231), before snap frozen in liquid nitrogen. The lentivirus expressing the desired GFP-tagged protein was added to the neuronal cultures between 5-8 days *in vitro* (DIV) to result in roughly 30-50% transduction efficiency.

Knockdown of βII-spectrin or clathrin heavy chain (CHC) by shRNA adenoviruses

The adenovirus expressing βII-spectrin shRNA was described previously (*41*). The adenovirus expressing CHC shRNA was purchased from SignaGen Laboratories. The adenoviruses expressing TrkB, FGFR1 or calpain-2 shRNA were purchased from Vector BioLabs. The adenovirus expressing a scramble shRNA sequence was used as a control (Vector BioLabs, 1122). The sense sequences of the βII-spectrin shRNA are 5'-GCATGTCACGATGTTACAA-3' and 5'-GGATGAAATGAAGGTGCTA-3' (*41*). The sense sequences of CHC shRNA, TrkB shRNA, FGFR1 shRNA, and calpain-2 shRNA are 5'-GTTGGTGACCGTTGTTATG-3' (*42*), 5'-CCACGGATGTTGCTGACCAAA-3', 5'-TGCCACCTGGAGCATCATAAT-3', and 5'-CGACGAGCTAATCATCGACTT -3', respectively. The adenoviruses were added to hippocampal neuronal cultures at DIV 2 for βII-spectrin knockdown and calpain-2 knockdown, at DIV 5 for TrkB knockdown and FGFR1 knockdown, and at DIV 7 for CHC knockdown.

Quantitative real-time PCR

Total RNA was extracted from neurons transfected by adenoviruses expressing scrambled shRNA, βII-spectrin shRNA, or CHC shRNA at DIV 20 using the Direct-zol MiniPrep kit (Zymo Research, R2050) according to the manufacturer's instructions. The quantitative PCR was performed on CFX Connect Real-Time PCR Detection System (Bio-Rad, Model: CFX Connect Optics Module) using the One-Step qRT-PCR Kit (Thermo Fisher Scientific, 11736059). The average relative mRNA levels of βII-spectrin and CHC versus the reference gene (βII-tubulin:) were determined among four biological replicates, each measured in three technical replicates. After the completion of PCR amplification, a melting curve was obtained for each target gene and these melting curves all generated a single amplicon, verifying a single PCR product. The sequences of PCR primers used were listed below.

βII-spectrin:

*Sptbn1*_Forward: 5'- TGGGAATACTTGCTGGAACTG -3'

*Sptbn1*_Reverse: 5'- ATTCACACCTCTTACACGCTC -3'

CHC:

*Cltc*_Forward: 5'- GCTGAACAAATACGAGTCCTTAG -3'

*Cltc*_Reverse: 5'- CCACAGATTTAACGAGATCACC -3'

βII-tubulin:

*Tubb2*_Forward: 5'-TGAGCATGGTATAGACCCCAC-3'

*Tubb2*_Reverse: 5'-ACCTGACTGAGTCCATTGTGC-3'

Treatment of neuronal cultures for ERK activation

The following drugs or ligands were used in this study: CB1 receptor agonist WIN 55,212-2 mesylate (Tocris, 1038), CB1 receptor antagonist SR141716A (SR; Tocris, 0923), PKC activator Phorbol 12,13-Dibutyrate (PDBu; Cell Signaling, 12808), recombinant Brain-Derived Neurotrophic Factor (BDNF; Alomone Labs, B-250), recombinant basic fibroblast growth factor (bFGF; Invitrogen, 13256029), MEK inhibitor U0126 (Cell Signaling, 9903S), calpain inhibitor MDL28170 (MDL; Santa Cruz Biotechnology, sc-201301), Latrunculin A (LatA; Santa Cruz Biotechnology, sc-202691), Cytochalasin D (CytoD; Santa Cruz Biotechnology, sc-201442), Src family kinase inhibitor PP2 (Santa Cruz Biotechnology, sc-202769), Trk inhibitor GNF5837 (Sigma, SML0844), and FGFR inhibitor PD173074 (Sigma, P2499).

Treatments were done for neuronal cultures between DIV 14-28. For ligand-induced ERK activation, neurons were treated with 250 nM WIN, 5 ng/µl NCAM1 antibody (NCAM1 Ab), 100 ng/µl BDNF, or 100 ng/µl bFGF at 37 °C. For NCAM1 Ab treatment, an additional 20-30 min pre-incubation step with NCAM1 Ab (5 ng/µl) at 4 °C was introduced to allow the antibody binding to NCAM1 at the cell surface, and the NCAM1 Ab treatment was initiated by subsequently transferring the neurons to 37 °C, as previously described (*26*). Inhibitors (20 µM U0126, 10 µM MDL, 2 µM PP2, 250 nM GNF5837, 250 nM PD173074) were added 10 min prior to the ligand addition (for WIN, BDNF, or bFGF treatment) or 10 min before the neurons were transferred to 37 °C (for NCAM1 Ab treatment). The CB1 antagonist SR (100 nM or 1 µM) was added 10 min prior to WIN addition. Pretreatment of 20 µM LatA and 50 µM CytoD was initiated 3 hr prior to WIN addition or 2.5 hr prior to NCAM1 Ab addition. These inhibitors and actin disrupting drugs were not removed during the ligand treatment. For direct PKC activation, 1 µM PDBu was added to neuronal cultures.

Fluorescence imaging for quantitative measurement of ERK phosphorylation and endocytosis

For quantitative measurement of ERK phosphorylation, cultured mouse hippocampal neurons at DIV 14-28 were fixed at different time points of ERK activation following the initiation of the ligand treatment. Neurons were fixed using 4% (w/v) paraformaldehyde (PFA) in phosphate buffered saline (PBS) containing 4% (w/v) sucrose for 20 min, washed three times in PBS, and incubated with ice-cold methanol for 30 min at -20°C. Neurons were then treated with 0.15% (v/v) Triton X-100 in PBS for 10 min and blocked in blocking buffer (PBS containing 3% (w/v) BSA) for 1 hr at room temperature, and subsequently stained with primary antibodies against phosphorylated ERK (pERK) in the blocking buffer overnight at 4 ºC. Neurons were next washed three times with PBS and incubated with Alexa-647-conjugated secondary antibody in the blocking buffer for 1 hr at RT.

For quantitative measurement of ligand-induced endocytosis, WIN was added to the cultured neurons at DIV 14-28. At different time points, neurons were washed quickly three times with PBS and fixed with 4% (w/v) PFA in PBS containing 4% (w/v) sucrose in PBS. Neurons were then treated with 0.15% (v/v) Triton and stained with the anti-CB1 primary antibody and secondary antibody as described above.

For imaging, we used a home-built microscope with an Olympus IX-71 body, a 20x (N.A. 0.85) or a 60x (N.A. 1.2) UPlanSApo objective (Olympus), and an EM-CCD camera (Andor iXon, DV885 KCS-VP, Andor Technology). Lumencor SOLA light engine (SOLA SE 5-LCR-SA) was used as the light source for illumination. The 20x objective was used for pERK imaging. The average pERK fluorescence was determined from 20-30 randomly selected imaging regions (400 μm × 400 μm each region) for each time point of ERK activation. The background fluorescence was subtracted and the average pERK fluorescence was normalized to the average fluorescence determined at the zero time point of ERK activation. For quantitative measurement of endocytosis, the 60x objective was used, and the fluorescence puncta of CB1 in neurons were identified as endosome signals and the average endosome density was determined from 20-30 randomly selected images.

Western blot and co-immunoprecipitation analyses

For immunoblotting of pERK, total ERK, pTrkB, total TrkB, pFGFR and total FGFR, cultured hippocampal neurons at DIV 14-28 were lysed in RIPA buffer containing 25mM Tris-HCl (pH 7.6), 150mM NaCl, 1% NP-40, 1% sodium deoxycholate, 0.1% SDS buffer (Thermo Fisher Scientific, 89900) complemented with 1x protease and phosphatase inhibitor cocktail (Thermo Fisher Scientific, 78440). Following centrifugation, the supernatants were collected as the whole-cell

lysates for Western blotting. The denatured protein mixtures in the whole-cell lysates were run on 4–15% gradient SDS-PAGE gels (Bio-rad, 4561086), transferred to polyvinylidene difluoride (PVDF) membranes (Thermo Fisher Scientific, LC2005), and immunoblotted using Pierce fast Western blot kit (Thermo Fisher Scientific, 35066) according to the manufacturer's instructions. Immunoreactivity of the Western blots was visualized using Sapphire Biomolecular Imager (Azure Biosystems, Model: SapphireRGBNIR).

Co-immunoprecipitation was performed as described previously (*21, 22*). Briefly, cultured hippocampal neurons were lysed in the co-immunoprecipitation lysis buffer containing 25 mM Tris-HCl (pH 7.4), 150 mM NaCl, 1% NP-40, 5% glycerol, 1x protease inhibitor cocktail (Thermo Fisher Scientific, 78440) on ice. For co-immunoprecipitation with CB1, NCAM1 and βII-spectrin, whole-cell lysates of these neurons were first pre-cleared with protein-G-coated beads conjugated with appropriate species IgGs (1 h, 4°C) and then incubated overnight with the CB1, NCAM1 or βII-spectrin antibody. Immunocomplexes were captured with protein-G-coated beads, rinsed five times with the co-immunoprecipitation lysis buffer, and eluted with Laemmli sample buffer (Bio-rad, 1610737). For immunoblotting of CB1, NCAM1, βII-spectrin, TrkB, and FGFR in the immunoprecipitates, immunoprecipitated proteins were denatured and run on 4–15% gradient SDS-PAGE gels (Bio-rad, 4561086), transferred to polyvinylidene difluoride (PVDF) membranes (Thermo Fisher Scientific, LC2005), and immunoblotted using Pierce fast Western blot kit (Thermo Fisher Scientific, 35066 and 35070) according to the manufacturer's instructions. Immunoreactivity of the Western blots was visualized using Sapphire Biomolecular Imager (Azure Biosystems, Model: SapphireRGBNIR).

Fluorescence labeling for STORM imaging

At 14-28 days *in vitro* (DIV), cultured mouse hippocampal neurons were fixed using 4% (w/v) PFA in PBS containing 4% (w/v) sucrose for 30 min, washed three times in PBS, and permeabilized with 0.15% (vol/vol) Triton X-100 in PBS for 10 min. For the two alternative cell fixation conditions shown in fig. S3, neurons were fixed with 3% (w/v) glyoxal or 4% PFA (w/v) and 0.2% (w/v) glutaraldehyde (GA) using the protocols described previously (*43, 44*). Neurons were then blocked in blocking buffer containing 3% (w/v) BSA in PBS for 1 hr at room temperature, and subsequently stained with primary antibodies in the blocking buffer overnight at 4 ºC. After incubation with primary antibodies, neurons were washed three times with PBS and stained with secondary antibodies in blocking buffer for 1 hr at room temperature.

For single-color STORM, neurons were immunostained for βII-spectrin, along with MAP2 as a dendritic marker. The secondary antibodies used for βII-spectrin was labeled with Alexa-647 for

STORM imaging. The secondary antibody used for MAP2 was conjugated with Alexa-488 or Cy3. To identify CB1- or NCAM1-positive axons/dendrites, CB1 or NCAM1 was co-stained with the corresponding primary antibody and a secondary antibody conjugated with Alexa-488 or Alexa-546. Only βII-spectrin was imaged using STORM, whereas MAP2, CB1 and NCAM1 were imaged using conventional fluorescence microscopy.

For two-color STORM, neurons were treated with WIN or NCAM1 Ab at room temperature for 5-10 min before PFA fixation. For NCAM1 Ab treatment, in contrast to WIN, an additional 20-30 min pre-incubation step with NCAM1 Ab at 4 °C was introduced to allow the antibody binding to NCAM1 at the cell surface, and the NCAM1 Ab treatment was initiated by subsequently transferring the neurons to room temperature, as previously described (*26*). The neurons were then immunostained for the indicated molecular pairs, using the secondary antibodies conjugated with CF680 and Alexa-647 for STORM imaging. For the two-color STORM imaging of RTKs and βII-spectrin, CB1 or NCAM1 was also co-stained with the corresponding primary antibody and an Alexa-546 conjugated secondary antibody, and imaged using conventional fluorescence microscopy to identify CB1- or NCAM1-positive axons. In the experiment testing the specificity of the observed WIN-induced effect to CB1, the CB1-specific antagonist SR (500 nM) was added 10 min prior to WIN addition, and was not removed during the WIN treatment.

STORM imaging

The STORM setup was built on an Olympus IX71 microscope with a 100x oil-immersion objective (Olympus, UPlanSApo, N.A. 1.4) and an EM-CCD camera (Andor iXon, DV887-DCS-BV, Andor Technology). 405-nm (Coherent, OBIS 405 LX 200 mW), 561-nm (Coherent, Sapphire 561-200 CW CDRH) and 640-nm (Coherent, Genesis MX 639-1000 STM) lasers were introduced into the sample through the back port of the microscope. The laser beams were shifted towards the edge of the objective so that the emerging light reached the sample at incidence angles slightly smaller than the critical angle of the glass-water interface, thus illuminating only the fluorophores within a few micrometers of the coverslip surface. ZT405/488/561/640rpc (Chroma) was used as the dichroic mirror and ZET405/488/561/640mv2 (Chroma) was used as the emission filter. For single-color 3D STORM imaging, Alexa-647 was imaged. For two-color STORM imaging, CF680 and Alexa-647 were imaged and a previously described ratiometric detection scheme (*45-47*) was used for detection. The fluorescence signal was split into two channels using a long-pass dichroic mirror (Chroma, T685lpxr) and the ratio between the signals in the two channels was used to determine the fluorophore identity (*45-47*). For single-color 3D STORM imaging, a cylindrical lens was

inserted into the detection path so that the images of single molecules turned elliptical and the *z* positions of the molecules could be determined from the ellipticity of the images (*20*).

The sample was imaged in PBS buffer containing 100 mM cysteamine (Sigma), 5% glucose (Sigma), 0.8 mg/mL glucose oxidase (Sigma), and 40 μg/mL catalase (Roche Applied Science). During imaging, continuous illumination of 640-nm laser (~2 kW/cm^2) was used to excite fluorescence from Alexa-647 and CF680 molecules and switched them into the dark state. Continuous illumination of the 405-nm laser (0-1 W/cm^2) was used to reactivate the fluorophores to the emitting state and the illumination power was controlled so that at any given instant, only a small, optically resolvable fraction of the fluorophores in the field of view were in the emitting state. A typical STORM image was generated from a sequence of about 30,000 image frames (for single-color STORM) or 55,000-60,000 frames (for two-color STORM) at a frame rate of 60 Hz. The recorded STORM movies were analyzed according to previously described methods (*20, 47*). Alexa-647 and CF680 molecules were differentiated by the ratio of intensities detected in the short and long wavelength channels (*45-47*). Super-resolution images were reconstructed from the molecular coordinates by depicting each location as a 2D Gaussian peak.

Correlation analysis of spatial distributions in STORM images

In single-color STORM experiments, one-dimensional (1D) autocorrelation analyses were used to measure the degree of periodicity of the MPS structure and quantify MPS degradation induced by ERK signaling. 1D autocorrelation analyses were performed on regions of axons or dendrites (~3 μm long) as previously described (*12*). Briefly, for each axonal or dendritic region, the localization distribution was projected to the long axis of the neurite segment to obtain a 1D distribution profile along the neurite, and the 1D autocorrelation function $AC(\Delta x)$ was calculated from the projected 1D distribution, using the following equation, $AC(\Delta x) = \frac{\sum_{x=1}^{N-\Delta x}(I(x)-\bar{I})(I(x+\Delta x)-\bar{I})}{\sum_{x=1}^{N}(I(x)-\bar{I})^2}$, where $\bar{I}$ is the average of $I(x)$, the projected 1D distribution of the signal, and Δx is the lag. The average 1D autocorrelation function was derived from 50-100 randomly selected axonal or dendritic regions for each condition, and the average 1D autocorrelation amplitude was defined as the difference between the first peak (at ± 190 nm) and the average of the two first valleys (at ± 95 nm and ± 285 nm, respectively) of the average autocorrelation function.

In the two-color STORM experiments, 1D cross-correlation analyses between the two different color channels were used to measure the degree of colocalization between a molecular pair in a periodic fashion, and were performed on regions of axons (~2 μm long.) For each axonal region, the localization distributions in the two color channels were each projected to the long axis of the

axon segment to obtain a 1D distribution profile along the axon, and the 1D cross-correlation function $CC(\Delta x)$ was calculated between the two projected 1D distributions, using the following equation, $CC(\Delta x) = \frac{\sum_{x=1}^{N-\Delta x}(I_1(x)-\bar{I}_1)(I_2(x+\Delta x)-\bar{I}_2)}{\sum_{x=1}^{N}(I_1(x)-\bar{I}_1)(I_2(x)-\bar{I}_2)}$, where $I_1(x)$ and $I_2(x)$ are the projected 1D distributions of the signals in the two color channels, $\bar{I}_1$ and $\bar{I}_2$ are the average values of $I_1(x)$ and $I_2(x)$, respectively, and Δx is the lag. The average 1D cross-correlation function was derived from 100-200 randomly selected axonal regions. The average 1D cross-correlation amplitude was defined as the difference between the average of the peaks at ± 190 nm and the average of the valleys at ± 95 and ± 285 nm, of the average 1D cross-correlation function. For directly measuring the colocalization between RTKs and RTK transactivators, the two-dimensional (2D) cross-correlation was also calculated between the 2D localization distributions in the two color-channels using the following equation, $CC(\Delta x, \Delta y) = \frac{\sum_{x=1}^{N-\Delta x}\sum_{y=1}^{M-\Delta y}(I_1(x,y)-\bar{I}_1)(I_2(x+\Delta x,y+\Delta y)-\bar{I}_2)}{\sum_{x=1}^{N}\sum_{y=1}^{M}(I_1(x,y)-\bar{I}_1)(I_2(x,y)-\bar{I}_2)}$, where $I_1(x,y)$ and $I_2(x,y)$ are the signals of the 2D localization distributions in the two color channels, $\bar{I}_1$ and $\bar{I}_2$ are the average values of $I_1(x,y)$ and $I_2(x,y)$, respectively, and Δx and Δy are the lags in the x and y directions, respectively. The average 2D cross-correlation amplitude (defined as the amplitude of the cross-correlation function at (0,0)) was derived from the 100-200 randomly selected axonal regions for each condition to determine the degree of colocalization. To get the baseline of average 2D cross-correlation amplitude due to molecules coming into proximity by random chance, the localization clusters in one of the two color-channels were identified using the Otsu threshold method (*48*) in each analyzed axonal region and then randomly redistributed within the axonal region, and the average 2D cross-correlation amplitude was calculated after this randomization.

SI references

40. C. Lois, E. J. Hong, S. Pease, E. J. Brown, D. Baltimore, Germline transmission and tissue-specific expression of transgenes delivered by lentiviral vectors. *Science* **295**, 868-872 (2002).
41. M. R. Galiano *et al.*, A Distal Axonal Cytoskeleton Forms an Intra-Axonal Boundary that Controls Axon Initial Segment Assembly. *Cell* **149**, 1125-1139 (2012).
42. S. Watanabe *et al.*, Clathrin regenerates synaptic vesicles from endosomes. *Nature* **515**, 228-233 (2014).
43. K. N. Richter *et al.*, Glyoxal as an alternative fixative to formaldehyde in immunostaining and super-resolution microscopy. *Embo Journal* **37**, 139-159 (2018).
44. K. A. K. Tanaka *et al.*, Membrane molecules mobile even after chemical fixation. *Nature Methods* **7**, 865-866 (2010).
45. M. Bossi *et al.*, Multicolor far-field fluorescence nanoscopy through isolated detection of distinct molecular species. *Nano Lett* **8**, 2463-2468 (2008).
46. C. M. Winterflood, E. Platonova, D. Albrecht, H. Ewers, Dual-color 3D superresolution microscopy by combined spectral-demixing and biplane imaging. *Biophys J* **109**, 3-6 (2015).
47. A. Gorur *et al.*, COPII-coated membranes function as transport carriers of intracellular procollagen I. *Journal of Cell Biology* **216**, 1745-1759 (2017).
48. N. Otsu, A Threshold Selection Method from Gray-Level Histograms. *IEEE Transactions on Systems, Man, and Cybernetics* **9**, 62 -66 (1979).

Supplementary Figures

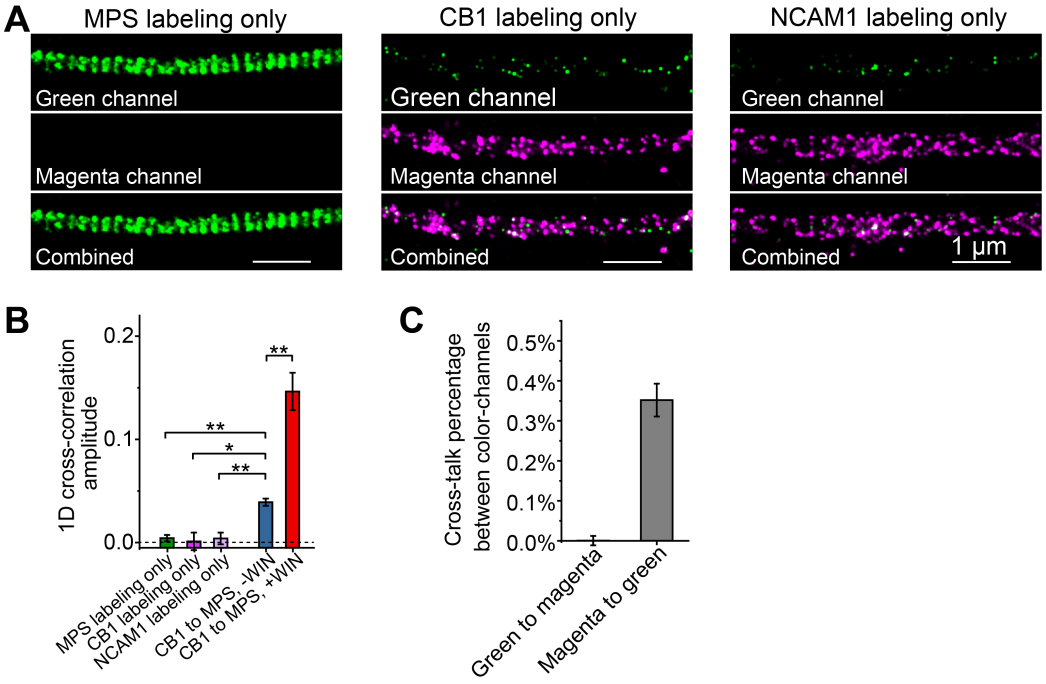

Fig. S1. Cross-talk analysis between the two color-channels of STORM. (A) Two-color STORM images of axons from untreated neurons immunostained only for βII-spectrin (green) (left, "MPS labeling only"), only for CB1 (middle, "CB1 labeling only"), and only for NCAM1 (right, "NCAM1 labeling only"). Scale bars: 1 μm. **(B)** Average 1D cross-correlation amplitudes between the two STORM color-channels for the three conditions described in (A), shown together with data obtain from two-color-labeled neurons (CB1 to MPS, -WIN and +WIN) reproduced from Fig. 1B for comparison. **: $P < 0.01$; actual P values (from left to right): 1.6×10^{-3}, 1.4×10^{-2}, 6.0×10^{-3}, 4.4×10^{-3}, (unpaired Student's t test). **(C)** Cross-talk percentages between the two STORM color-channels determined from the single-color-labeled neurons shown in (A). The green-to-magenta percentage was derived from neurons immunostained only for βII-spectrin and the magenta-to-green percentage was derived from both neurons immunostained only for CB1 and neurons immunostained only for NCAM1. Data in the bar graphs are mean ± s.e.m. (n = 3 biological replicates; 100-200 axonal regions were examined per condition).

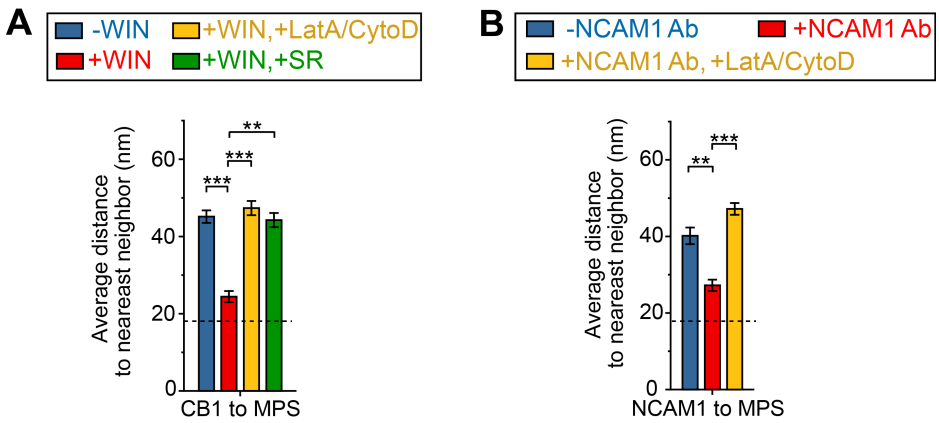

Fig. S2. Average nearest-neighbor distance analysis between CB1/NCAM1 and the MPS during RTK transactivation. **(A)** Average distances of CB1 localization clusters to nearest-neighbor βII-spectrin localization clusters under the four conditions as described in Fig. 1, A and B. Data are mean ± s.e.m. (n = 3 biological replicates; 100-200 axonal regions were examined per condition). **: $P < 0.01$; ***: $P < 0.001$; actual P values (from left to right): 6.8×10^{-4}, 6.2×10^{-4}, 1.1×10^{-3} (unpaired Student's t test). **(B)** Average distances of NCAM1 localization clusters to nearest-neighbor βII-spectrin localization clusters under the three conditions as described in Fig. 1, C and D. Data are mean ± s.e.m. (n = 3 biological replicates; 100-200 axonal regions were examined per condition). **: $P < 0.01$; ***: $P < 0.001$; actual P values (from left to right): 7.3×10^{-3}, 7.2×10^{-4} (unpaired Student's t test). Note that because both the protein targets and the antibodies used to label the target proteins have finite sizes, we do not anticipate this distance to become zero even for two contacting protein molecules. The dashed line (at ~17 nm) represents a crude baseline estimation of the average nearest-neighbor distance between fluorophores that are associated with two contacting protein molecules through immunostaining using primary and the secondary antibodies. This crude baseline estimation was obtained by simulation, assuming that the primary antibody binding sites on the two contacting protein molecules are separate by ~5 nm (to approximate the typical size of target proteins), that primary and secondary antibody molecules each have a size of ~15 nm, binding to their respective target in any orientation with equal probability, the secondary antibody could bind to any site on the primary antibody, and that the fluorophores can be attached to any site of the secondary antibody with equal possibility. An alternative way to approximate this baseline distance simply by calculating $\sqrt{5^2 + 15^2 + 15^2}$ generates a similar number (~22 nm). We further note that because each localization cluster includes multiple localizations, the uncertainty in determining the cluster centroid position is relatively small and hence would not significantly change this estimation if this localization uncertainty is taken into account.

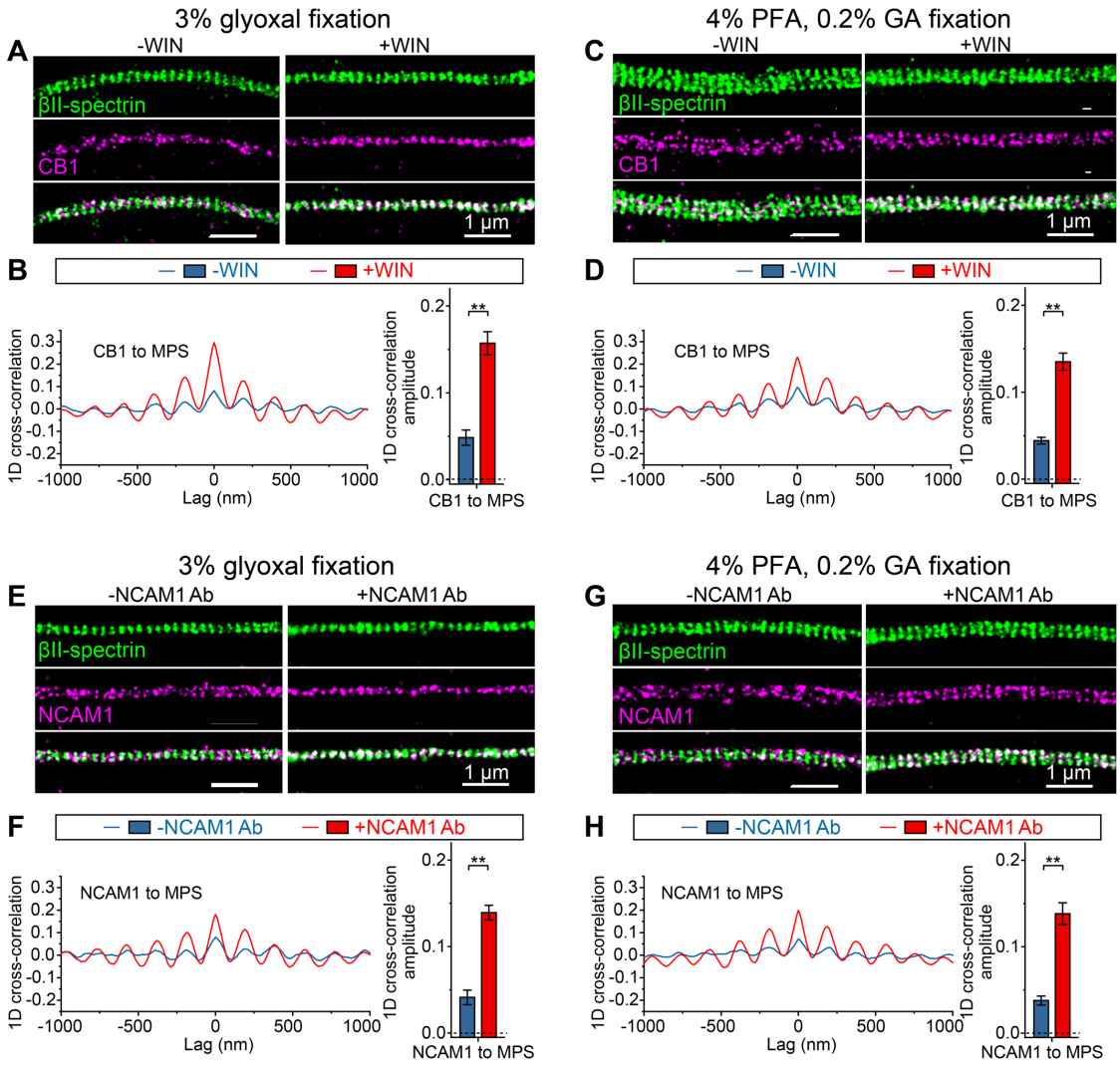

Fig. S3. Spatial relationship between CB1/ NCAM1 and the MPS under two alterative fixation conditions. (A) Two-color STORM images of βII-spectrin (green) and CB1 (magenta) in the axons of untreated neurons (left, "-WIN") and neurons treated with WIN for 10 min (right, "+WIN"), which were fixed with 3% glyoxal instead of our standard fixative (4% paraformaldehyde (PFA)). **(B)** Average 1D cross-correlation functions and 1D cross-correlation amplitudes between the distributions of CB1 and βII-spectrin for the two conditions described in (A). Data are mean ± s.e.m. (n = 3 biological replicates; 100-200 axonal regions were examined per condition). **: $P < 0.01$; actual P value: 2.4×10^{-3} (unpaired Student's t test). **(C, D)** Same as (A, B) but the neurons were fixed with 4% PFA and 0.2% glutaraldehyde (GA). **: $P < 0.01$; actual P value: 1.1×10^{-3} (unpaired Student's t test). **(E-H)** Similar to (A-D) but for βII-spectrin and NCAM1 instead of βII-spectrin and CB1, before and 10 min after the initiation of NCAM1 Ab treatment. **: $P < 0.01$; actual P values: 1.1×10^{-3} (F), 1.8×10^{-3} (H); unpaired Student's t test. WIN and NCAM1 Ab treatments are as described in Fig. 1.

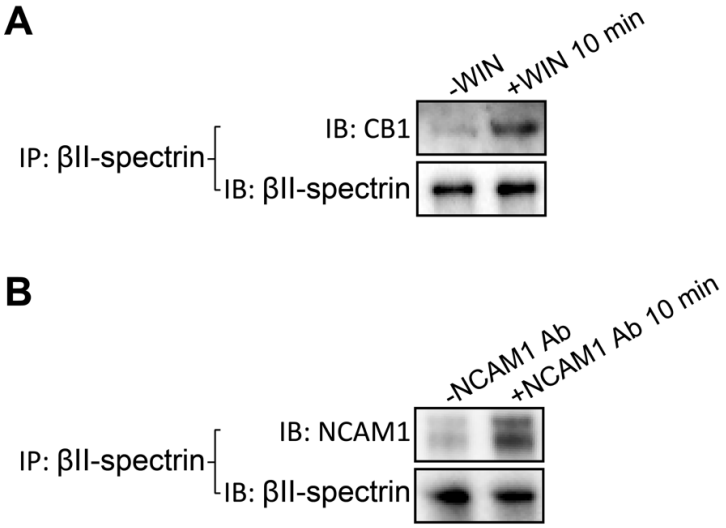

Fig. S4. Co-immunoprecipitation analysis of ligand-induced interactions between CB1/NCAM1 and the MPS. (A) Immunoblotting (IB) for CB1 and βII-spectrin of the protein complexes immunoprecipitated (IP) by βII-spectrin antibody from whole-cell lysates of neurons before or 10 min after treatment with WIN. **(B)** Immunoblotting (IB) for NCAM1 and βII-spectrin of the protein complexes immunoprecipitated (IP) by βII-spectrin antibody from whole-cell lysates of neurons before ("-NCAM1 Ab) or 10 min after ("+NCAM1 Ab") the initiation of NCAM1 Ab treatment. As described in Fig. 1, the same amount of NCAM1 Ab was added to the neurons in the preincubation step at 4 ℃ for both "-NCAM1 Ab" and "+NCAM1 Ab 10 min" conditions to allow antibody binding and unbound NCAM1 Ab was washed away. The temperature was then increased to initiate the NCAM1 Ab treatment in "+NCAM1 Ab 10 min" condition to induce signaling. Therefore, although the protein G-coated beads used to capture the βII-spectrin antibody added to the whole-cell lysate may also capture the small amount of NCAM1 antibody remained in the lysate, and pulled down some NCAM1 through this alternative mechanism, the amount of NCAM1 pulled down through this mechanism should be similar under both conditions. Hence the substantial increase in the amount of co-immunoprecipitated NCAM1 observed in the "+NCAM1 Ab 10 min" condition is most likely due to interaction with βII-spectrin induced by ligand stimulation. Western blots are representative examples from two independent biological replicates.

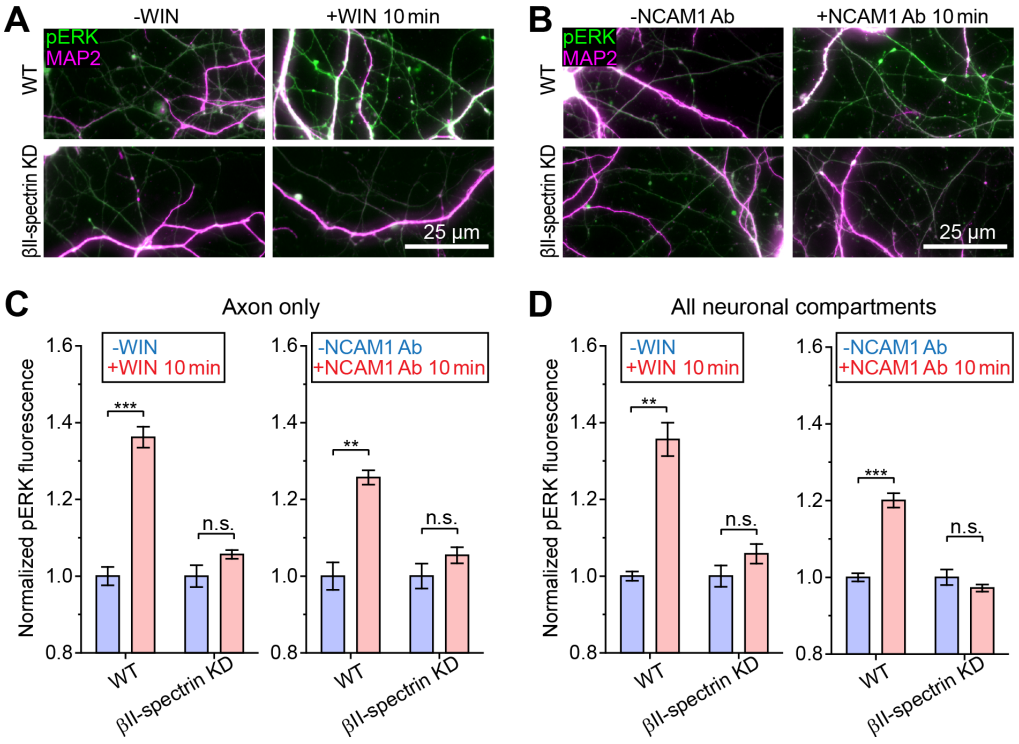

Fig. S5. Ligand-induced ERK activation in neurons. (A) Immunofluorescence images of phosphorylated (activated) ERK (pERK, green) and the dendritic marker MAP2 (magenta) in wild type (WT, top) and βII-spectrin knockdown (βII-spectrin KD, bottom) neurons that were untreated (left) or treated with WIN for 10 min (right). **(B)** Same as (A) but for neurons that are either before (left) or 10 min after the initiation of NCAM1 Ab treatment (right). NCAM1 Ab treatment was initiated by a temperature increase step, as described in Fig. 2B. Scale bars: 25 μm. **(C)** Quantification of pERK signal in axons (MAP2-negative neurites) before and after ligand (WIN or NCAM1 Ab) treatment in WT and βII-spectrin KD neurons. Blue: before ligand treatment. Red: after ligand treatment. **: $P < 0.01$; ***: $P < 0.001$; n.s.: not significant ($P > 0.1$); actual P values (from left to right): 5.6×10^{-4}, 0.14, 3.2×10^{-3}, 0.23 (unpaired Student's t test). **(D)** Quantification of pERK signal from all neuronal compartments before and after ligand treatment. The signals are normalized to the values obtained before ligand treatment. **: $P < 0.01$; ***: $P < 0.001$; n.s.: not significant ($P > 0.1$); actual P values (from left to right): 1.4×10^{-3}, 0.20, 7.5×10^{-4}, 0.17 (unpaired Student's t test). Data in (C) and (D) are mean ± s.e.m. ($n = 3$ biological replicates; 20-30 imaged regions were examined per condition).

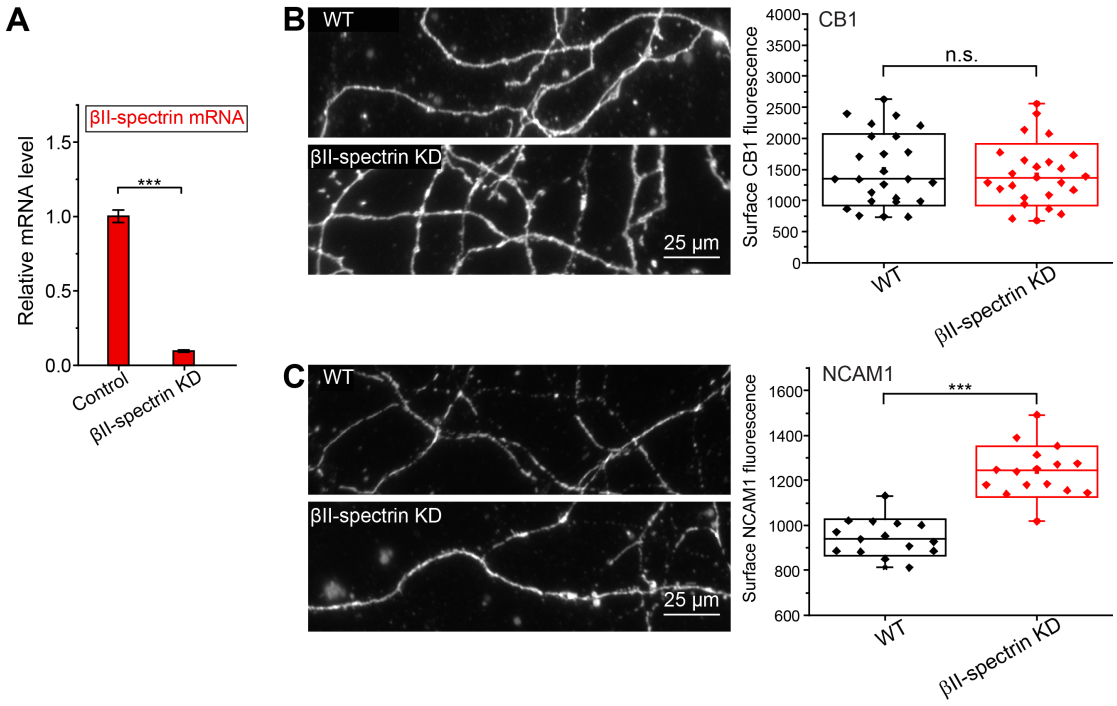

Fig. S6. Cell-surface expression of CB1 and NCAM1 in WT and βII-spectrin KD neurons. (A) Quantitative RT-PCR results indicating the normalized mRNA expression levels of βII-spectrin determined for neurons transfected with adenoviruses expressing scrambled shRNA (control) or βII-spectrin shRNA. ***: $P < 0.001$; actual P value: 2.9×10^{-5} (unpaired Student's t test).. Data are mean ± s.e.m. ($n = 3$ biological replicates). **(B)** Left: Fluorescence image of cell-surface CB1 for WT (top panel) and βII-spectrin KD (bottom panel) neurons. Right: Box plot of the cell-surface CB1 expression in WT (black) and βII-spectrin KD (red) neurons. n.s.: not significant ($P > 0.1$); actual P value: 0.61 (unpaired Student's t test). **(C)** Left: Fluorescence image of cell-surface NCAM1 for WT (top panel) and βII-spectrin KD (bottom panel) neurons. Right: Box plot of the surface NCAM1 expression in the WT (black) and βII-spectrin KD (red) neurons. ***: $P < 0.001$; actual P value: 4.3×10^{-9} (unpaired Student's t test). Box plot elements: the line in the middle of the box indicates the median value; the upper and lower bounds of the box indicate standard deviation; the whiskers indicate the maximum and minimum. For staining the cell-surface CB1 and NCAM1, the primary antibody detecting the extracellular domain of CB1 or NCAM1 was added to live neuronal cultures for 10 min at room temperature, followed by 4% PFA fixation and incubation with Alexa-546 conjugated secondary antibodies. Scale bars: 25 μm. .

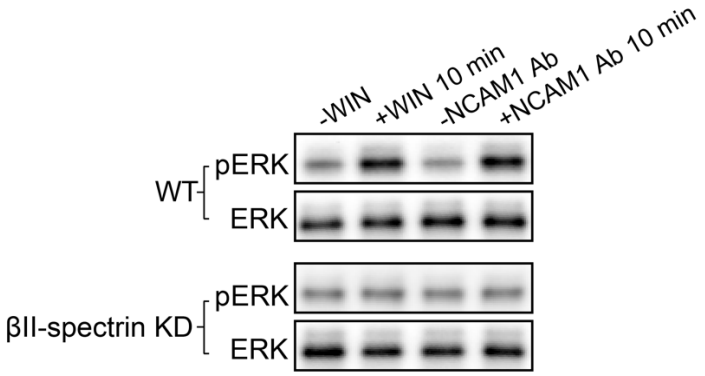

Fig. S7. Western blot analysis of ligand-induced ERK activation. Western blotting for phosphorylated (activated) ERK (pERK) and total ERK in whole-cell lysates from wild type (WT) neurons (top) and βII-spectrin KD neurons (bottom) before or 10 min after the initiation of WIN or NCAM1 Ab treatment. Western blots are representative examples from two independent biological replicates.

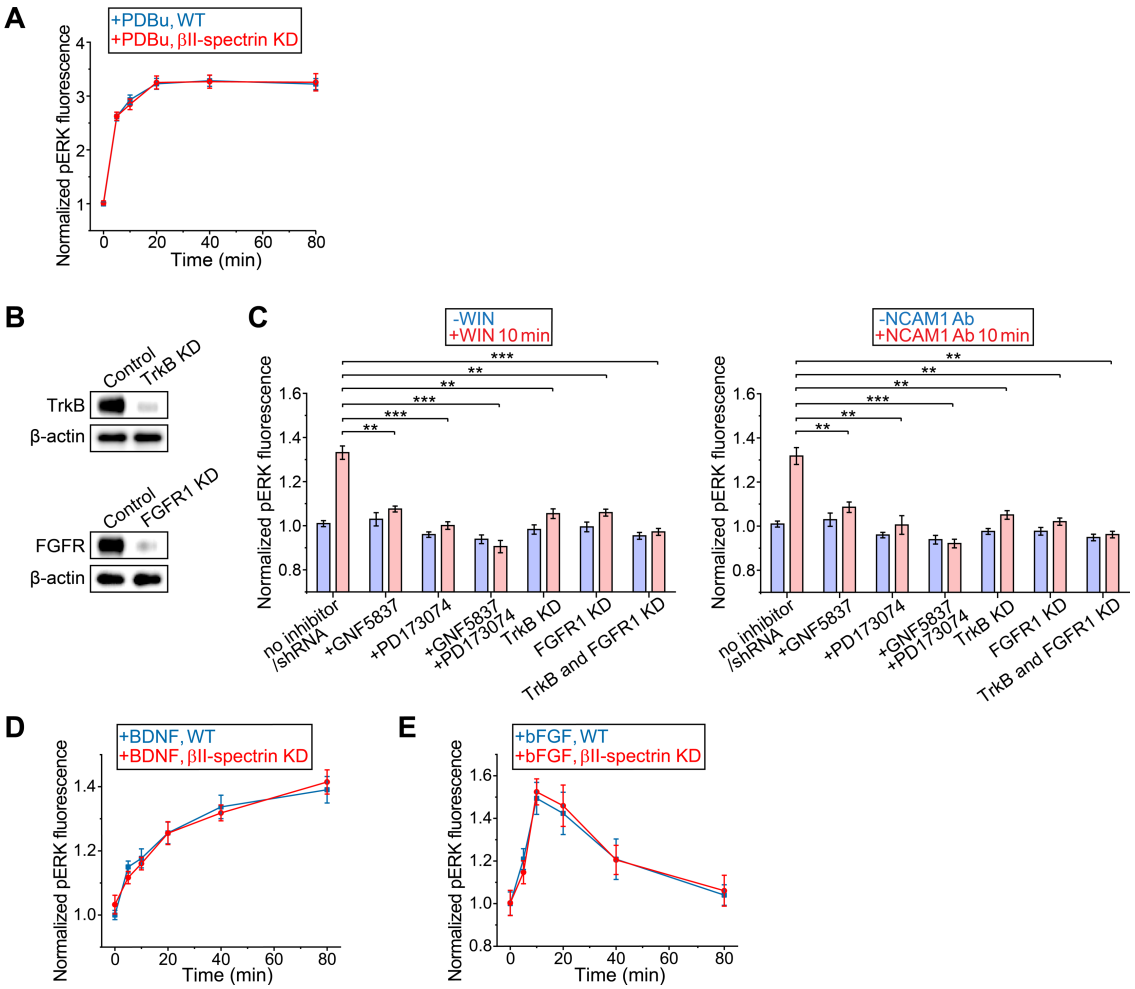

Fig. S8. Additional analyses of ERK signaling induced by direct PKC, TrkB and FGFR activation or by TrkB and FGFR transactivation. (A) Time courses of ERK activation upon addition of PDBu, a PKC activating drug, for WT and βII-spectrin KD neurons. Data are mean ± s.e.m. (n = 3 biological replicates; 20-30 imaged regions were examined per condition). **(B)** Western blots showing the knockdown of TrkB and FGFR1 in the cultured neurons treated with TrkB and FGFR1 shRNA, respectively. The shRNAs were introduced by adenoviruses. Western blots are representative examples from two independent biological replicates. **(C)** Left: Quantification of pERK fluorescence before (blue) and 10 min after (red) addition of the CB1 ligand WIN to neurons in the absence and presence of TrkB inhibitor GNF5837 (IC_{50} = 9 nM for TrkB), FGFR inhibitor PD173074 (IC_{50} = 25 nM for FGFR1), or both inhibitors, as well as to neurons treated with TrkB shRNA, FGFR1 shRNA, or both shRNAs. Right: Same as (Left) but for NCAM1 Ab treatment instead of WIN treatment. Data from untreated neurons are reproduced in both plots to facilitate comparison. Data are mean ± s.e.m. (n = 3 biological replicates; 20-30 imaged regions were examined per condition). **: $P < 0.01$; ***: $P < 0.001$; actual P values (from left to right): 1.5×10^{-3}, 6.9×10^{-4}, 4.9×10^{-4}, 1.8×10^{-3}, 1.3×10^{-3}, 5.0×10^{-4}, 6.7×10^{-3}, 5.0×10^{-3}, 7.6×10^{-4}, 3.4×10^{-3}, 2.0×10^{-3}, 1.0×10^{-3} (unpaired Student's t test). **(D and E)** Time courses of ERK activation upon addition of BDNF, a TrkB ligand (D), and bFGF, a FGFR ligand (E), in WT (blue) and βII-spectrin KD (red) neurons. Data are mean ± s.e.m. (n = 3 biological replicates; 20-30 imaged regions were examined per condition).

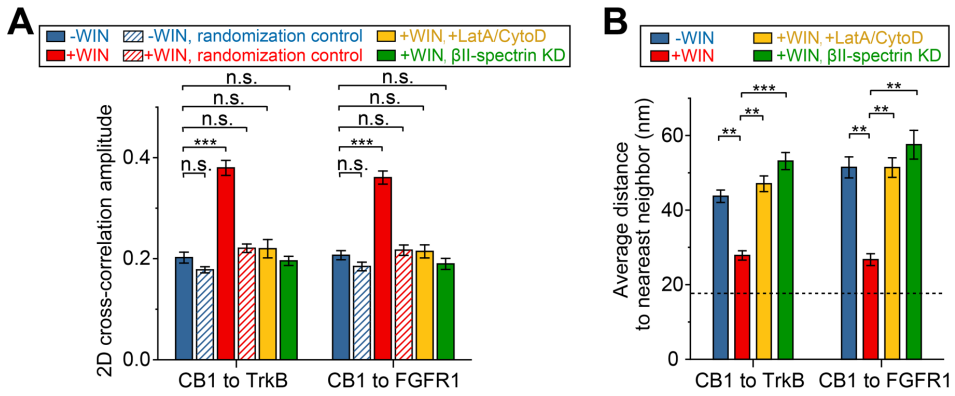

Fig. S9. Additional analyses of the spatial relationship between CB1 and RTKs during CB1-mediated RTK transactivation. **(A)** Average 2D cross-correlation amplitudes between the distribution of CB1 and the distributions of RTKs (TrkB or FGFR1) from many CB1-positive axons under four conditions (Blue: untreated neurons; Red: neurons treated with WIN; Yellow: neurons treated with LatA and CytoD prior to WIN treatment; Green: βII-spectrin KD neurons treated with WIN). The 2D cross-correlation amplitude was defined as the amplitude of the 2D cross-correlation function at 0-nm shift between the CB1 and RTK channels. The cross-correlation amplitudes for random-chance colocalization were also determined by randomizing the spatial distributions of CB1 molecules for the -WIN (blue hashed) and +WIN (red hashed) conditions. ***: $P < 0.001$; n.s.: not significant ($P > 0.1$); actual P values (from left to right): 0.12, 6.4×10^{-4}, 0.24, 0.45, 0.67, 0.15, 6.2×10^{-4}, 0.51, 0.66, 0.29 (unpaired Student's t test). **(B)** Average distances of CB1 localization clusters to nearest-neighbor TrkB localization clusters and average distances of CB1 localization clusters to nearest-neighbor FGFR localization clusters (Blue: untreated neurons; Red: neurons treated with WIN; Yellow: neurons treated with LatA and CytoD prior to WIN treatment; Green: βII-spectrin KD neurons treated with WIN). The dashed line (~17 nm) represents the baseline estimation for two contacting proteins labeled with primary and secondary antibodies, as described in fig. S2. **: $P < 0.01$; ***: $P < 0.001$; actual P values (from left to right): 1.6×10^{-3}, 1.4×10^{-3}, 6.4×10^{-4}, 1.6×10^{-3}, 1.3×10^{-3}, 1.8×10^{-3} (unpaired Student's t test). Data are mean ± s.e.m. ($n = 3$ biological replicates; 100-200 axonal regions were examined per condition).

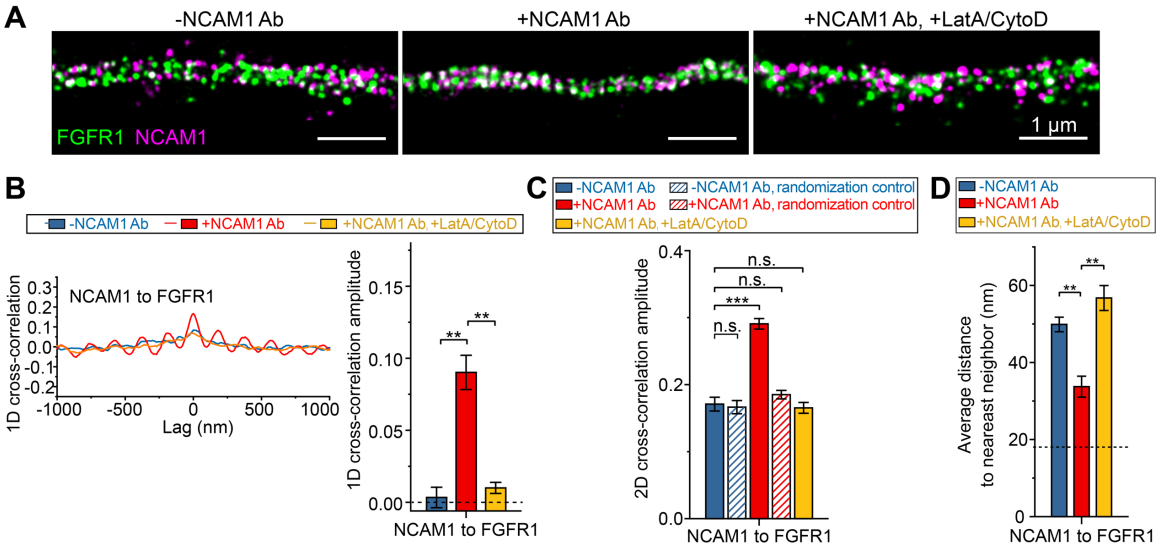

Fig. S10. Spatial relationship between FGFR1 and NCAM1 during NCAM1-mediated transactivation of FGFR1. (A) Two-color STORM images of FGFR1 (green) and NCAM1 (magenta) in the axons of neurons before the initiation of NCAM1 Ab treatment (left, "-NCAM1 Ab"), neurons 10 min after the initiation of NCAM1 Ab treatment (middle, "+NCAM1 Ab"), and neurons pretreated with LatA and CytoD prior to NCAM1 Ab treatment (right, "+NCAM1 Ab, +LatA/CytoD"). NCAM1 Ab treatment was performed as described in Fig. 1C. NCAM1 was visualized by immunostaining with NCAM1 antibody, and FGFR1 was visualized by moderate expression of GFP-tagged FGFR1 through low-titer lentiviral transfection and detection through GFP antibody. Scale bars: 1 μm. **(B)** Left: Average 1D cross-correlation functions between the distributions of FGFR1 and NCAM1 from many NCAM1-positive axons for the three conditions as in (A**)**. Right: The average 1D cross-correlation amplitudes for the three conditions. Blue: -NCAM1 Ab; Red: +NCAM1 Ab; Yellow: +NCAM1 Ab, +LatA/CytoD. **: $P < 0.01$; actual P values (from left to right): 3.3×10^{-3}, 3.0×10^{-3} (unpaired Student's t test). **(C)** Average 2D cross-correlation amplitudes between the distribution of NCAM1 and FGFR1 from many NCAM1-positive axons for the three conditions as in (A). The 2D cross-correlation amplitudes are as described in fig. S9A. Blue: -NCAM1 Ab; Red: +NCAM1 Ab; Yellow: +NCAM1 Ab, +LatA/CytoD. The cross-correlation amplitudes for random-chance colocalization were also determined by randomizing the spatial distributions of NCAM1 molecules for the -NCAM1 Ab (blue hashed) and +NCAM1 Ab (red hashed) conditions. ***: $P < 0.001$; n.s.: not significant ($P > 0.1$); actual P values (from left to right): 0.76, 7.6×10^{-4}, 0.31, 0.69 (unpaired Student's t test). **(D)** Average distances of NCAM1 localization clusters to nearest-neighbor FGFR1 localization clusters under the three indicated conditions (Blue: -NCAM1 Ab; Red: +NCAM1 Ab; Yellow: +NCAM1 Ab, +LatA/CytoD). The dashed line (~17 nm) represents the baseline estimation for two contacting proteins labeled with primary and secondary antibodies, as described in fig. S2. **: $P < 0.01$; actual P values (from left to right): 8.2×10^{-3}, 5.5×10^{-3} (unpaired Student's t test). Data in bar graphs are mean ± s.e.m. (n = 3 biological replicates; 100-200 axonal regions were examined per condition).

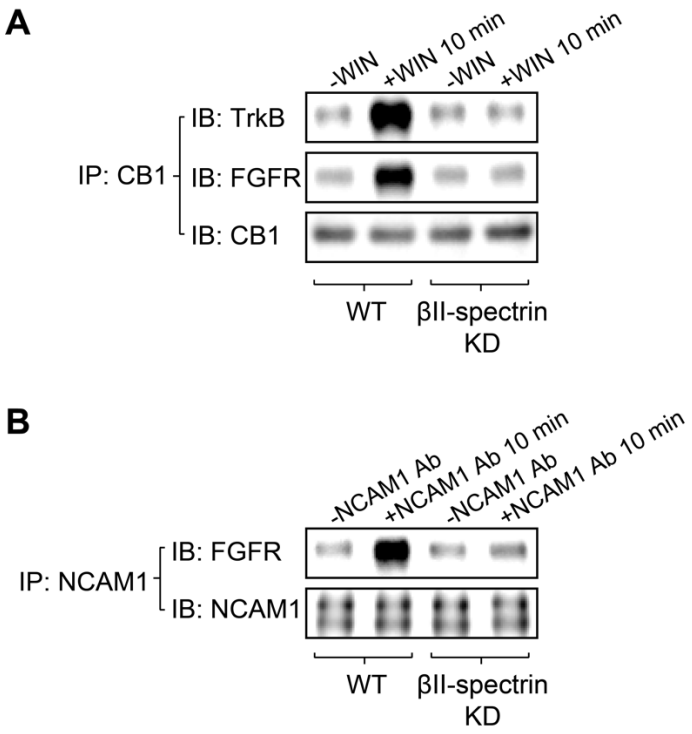

Fig. S11. Co-immunoprecipitation analysis of ligand-induced interactions between CB1/ NCAM1 and RTKs. (A) Immunoblotting (IB) for TrkB, FGFR and CB1 of the protein complexes immunoprecipitated (IP) by CB1 antibody from whole-cell lysate of wild type (WT) and βII-spectrin knockdown (KD) neurons untreated or treated with WIN for 10 min. **(B))** Immunoblotting (IB) for FGFR and NCAM1 of the protein complexes immunoprecipitated (IP) by NCAM1 antibody from whole-cell lysate of WT and βII-spectrin KD neurons before or 10 min after the initiation of NCAM1 Ab treatment. Western blots are representative examples from two independent biological replicates.

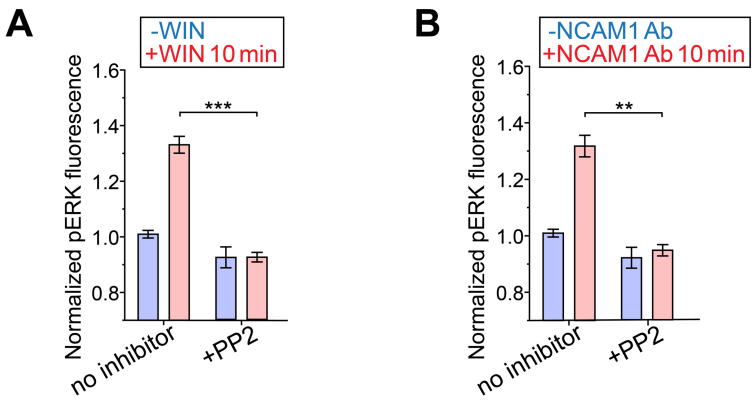

Fig. S12. Effect of the Src-family kinase inhibitor PP2 on ligand-induced ERK activation. (A) Quantification of pERK fluorescence before (blue) and 10 min after (red) addition of the CB1 ligand WIN in the absence and presence of the Src-family kinase inhibitor PP2 (IC_{50} = 1.4 µM for Src and 5 nM for Fyn). ***: $P < 0.001$; actual P value: 3.1×10^{-4} (unpaired Student's t test). **(B)** Quantification of pERK fluorescence before (blue) and 10 min after (red) initiating the NCAM1 Ab treatment in the absence and presence of PP2. **: $P < 0.01$; actual P value: 1.1×10^{-3} (unpaired Student's t test). Data are mean ± s.e.m. (n = 3 biological replicates; 20-30 imaged regions were examined per condition). The data in fig. S8C (no inhibitor condition) were reproduced here for comparison.

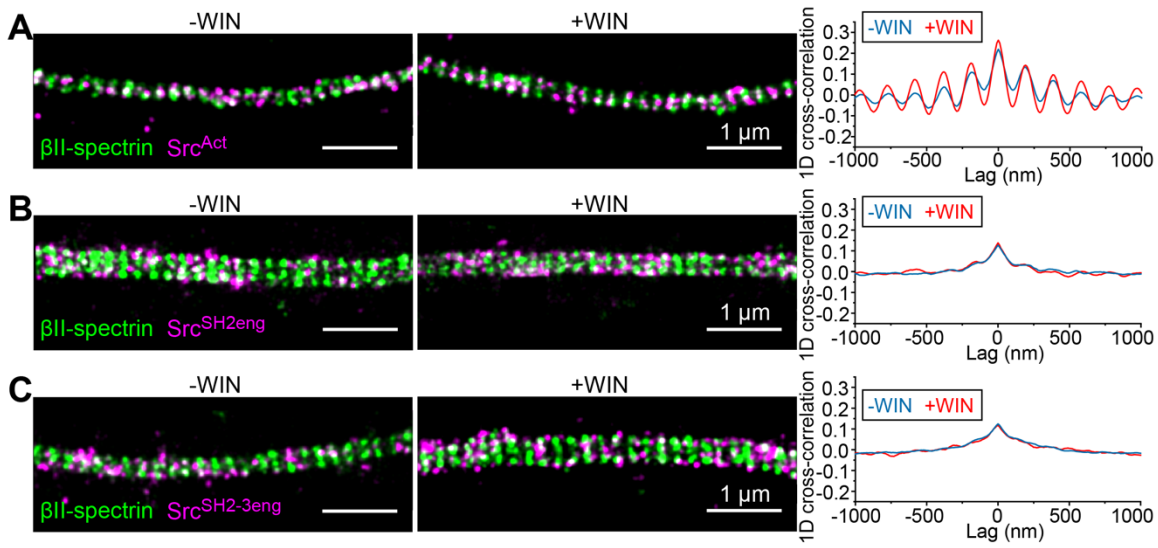

Fig. S13. Spatial relationship between the MPS and the activity mutants of Src during CB1-mediated RTK transactivation. (A) Left: Two-color STORM images of βII-spectrin (green) and Src^{Act} (magenta) in CB1-positive axons of untreated neurons (-WIN) and neurons treated with WIN for 10 min (+WIN). Scale bars: 1 μm. Right: Corresponding average 1D cross-correlation functions of the βII-spectrin and Src^{Act} distributions from many CB1-positive axons for these two conditions (Blue: -WIN; Red: +WIN). **(B)** Same as in (A), but for Src^{SH2eng} instead of Src^{Act}. **(C)** Same as in (A), but for $Src^{SH2-3eng}$ instead of Src^{Act}. βII-spectrin was immunostained with an antibody against the C-terminus of βII-spectrin, and the Src mutants were visualized by expression of GFP-tagged Src^{Act}, Src^{SH2eng}, or $Src^{SH2-3eng}$ through low-titer lentiviral transfection and detection through GFP antibody.

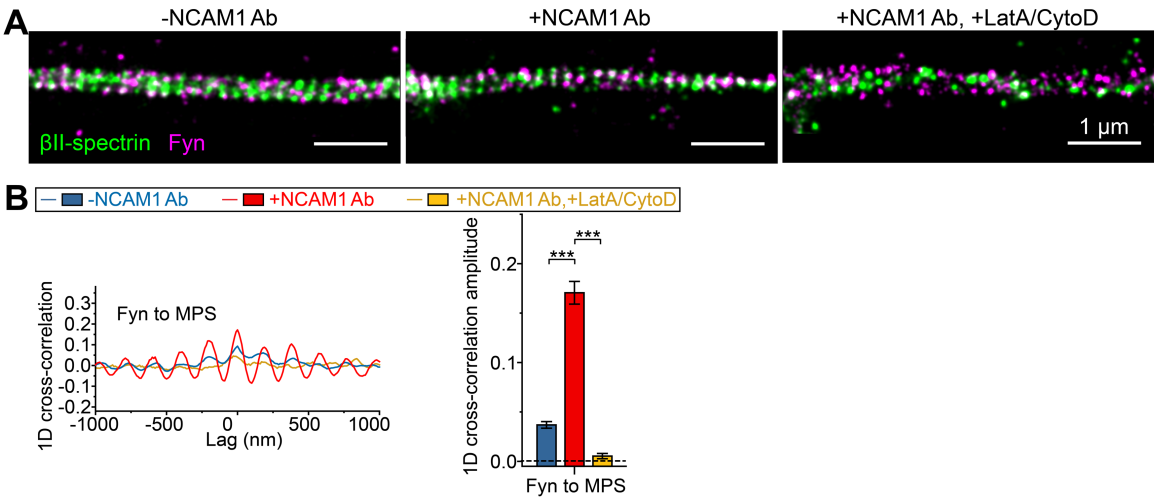

Fig. S14. Spatial relationship between the Src-family kinase, Fyn, and the MPS during NCAM1-mediated RTK transactivation. (A) Two-color STORM images of βII-spectrin (green) and Fyn (magenta) in NCAM1-positive axons of neurons before initiation of NCAM1 Ab treatment (left, "-NCAM1 Ab"), neurons 10 min after initiation of NCAM1 Ab treatment (middle, "+NCAM1 Ab"), and neurons pretreated with LatA and CytoD prior to NCAM1 Ab treatment (right, "+NCAM1 Ab, +LatA/CytoD"). βII-spectrin was immunostained with an antibody against the C-terminus of βII-spectrin, and Fyn was visualized by expression of GFP-tagged Fyn through low-titer lentiviral transfection and detection through GFP antibody. Scale bars: 1 μm. **(B)** Left: Average 1D cross-correlation functions between the distributions of βII-spectrin and Fyn from many NCAM1-positive axons for the three conditions described in (A). Right: Average 1D cross-correlation amplitudes for the three conditions. Blue: -NCAM1 Ab; Red: +NCAM1 Ab; Yellow: +NCAM1 Ab, +LatA/CytoD. Data are mean ± s.e.m. (n = 3 biological replicates; 100-200 axonal regions were examined per condition). ***: $P < 0.001$; actual P values (from left to right): 3.6×10^{-4}, 1.5×10^{-4} (unpaired Student's t test).

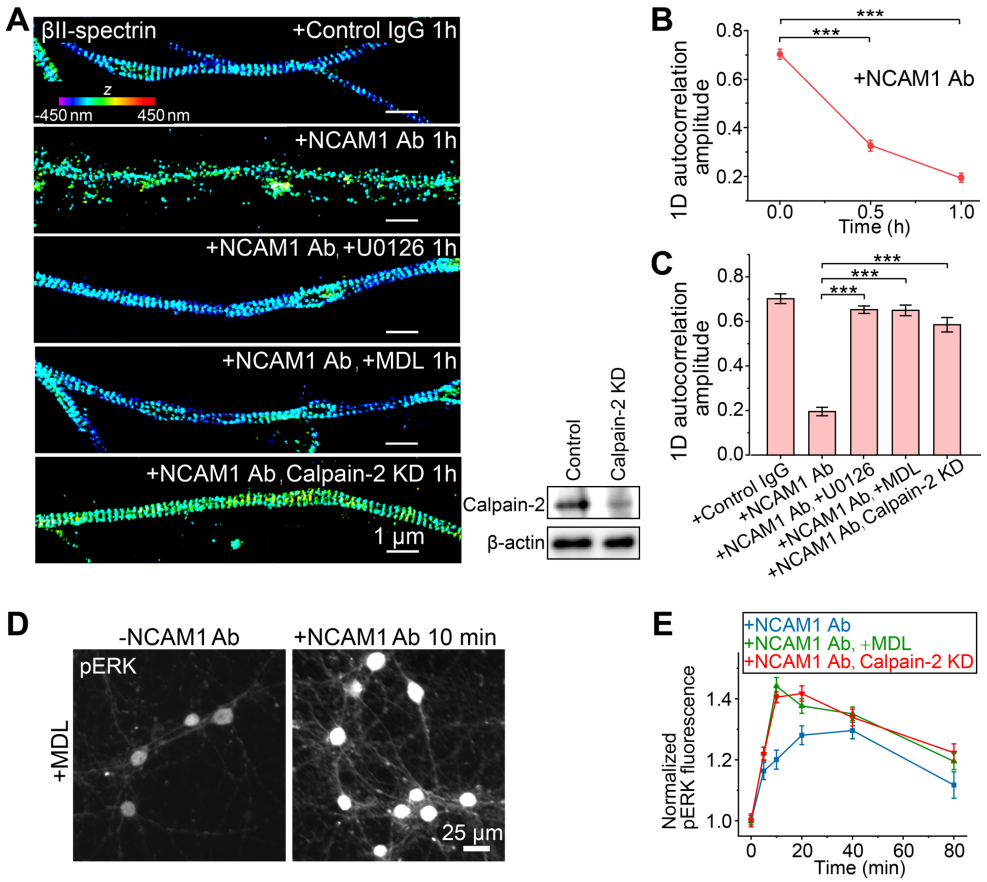

Fig. S15. NCAM1-mediated ERK signaling causes degradation of the MPS structure, providing a negative feedback for signaling. (A) Left: 3D STORM images of βII-spectrin in NCAM1-positive axons of neurons treated with control IgG that does not bind NCAM1, neurons treated with NCAM1 Ab for 1 hr in the absence and presence of the MEK inhibitor U0126 or the calpain inhibitor MDL, and caplain-2 knockdown neurons treated with NCAM1 Ab for 1 hr. Scale bars: 1 μm. Colored scale bar indicates the z-coordinate information. Right: Western blots showing the knockdown of calpain-2 in the cultured neurons treated with adenovirus expressing calpain-2 shRNA. Western blots are representative examples from two independent biological replicates. **(B)** Average 1D auto-correlation amplitude of the βII-spectrin distribution, indicating the degree of the periodicity in the MPS structure, for NCAM1-positive axons at different time points after initiating the NCAM1 Ab treatment. Data are mean ± s.e.m. (n = 3 biological replicates; 50-100 axonal regions were examined per condition). ***: $P < 0.001$; actual P values (from left to right): 1.8×10^{-4}, 6.2×10^{-5} (unpaired Student's t test). **(C)** Average 1D auto-correlation amplitudes obtained for the five conditions described in (A). Data are mean ± s.e.m. (n = 3 biological replicates; 50-100 axonal regions were examined per condition). ***: $P < 0.001$; actual P values (from left to right): 5.6×10^{-5}, 1.2×10^{-4}, 4.9×10^{-4} (unpaired Student's t test). **(D)** Immunofluorescence images of pERK in neurons pretreated with MDL, before (left) and 10 min after (right) initiating the NCAM1 Ab treatment. Scale bars: 25 μm. **(E)** Time courses of ERK activation after initiating the NCAM1 Ab treatment for control neurons (blue, "+NCAM1 Ab"), neurons pretreated with MDL (green, "+NCAM1 Ab, +MDL"), and calpain-2 knockdown neurons (red, "+NCAM1 Ab, Calpain-2 KD"). The curve for control neurons is reproduced from Fig. 2C. Data are mean ± s.e.m. (n = 3 biological replicates; 20-30 imaging regions were examined per condition).

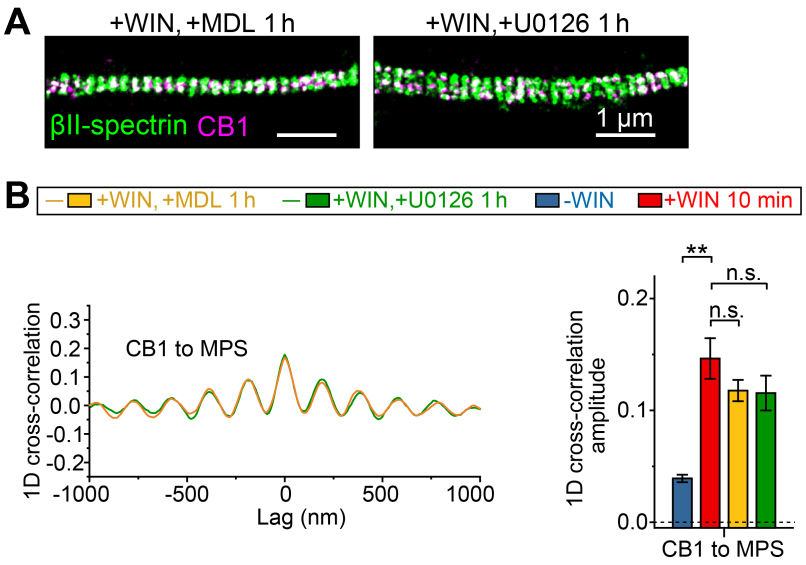

Fig. S16. Spatial relationship between CB1 and the MPS upon ligand treatment in the presence of calpain and MEK inhibitors. (A) Two-color STORM images of βII-spectrin (green) and CB1 (magenta) in the axons of neurons treated with WIN for 1 hr in the presence of the calpain inhibitor MDL (+WIN, +MDL) or the MEK inhibitor U0126 (+WIN, +U0126). Scale bars: 1 μm. **(B)** Average 1D cross-correlation functions (left) and 1D cross-correlation amplitudes (right) between the distributions of βII-spectrin and CB1 from many CB1-positive axons for the two conditions described in (A). Yellow: neurons treated with WIN in the presence of MDL; Green: neurons treated with WIN in the presence of U0126. The cross-correlation amplitudes obtained under -WIN (blue) and +WIN (red) conditions, reproduced from Fig. 1B, are shown together for comparison. Data in the bar graphs are mean ± s.e.m. (n = 3 biological replicates; 100-200 axonal regions were examined per condition). **: $P < 0.01$; n.s.: not significant ($P > 0.1$); actual P values (from left to right): 4.4×10^{-3}, 0.24, 0.27 (unpaired Student's t test).

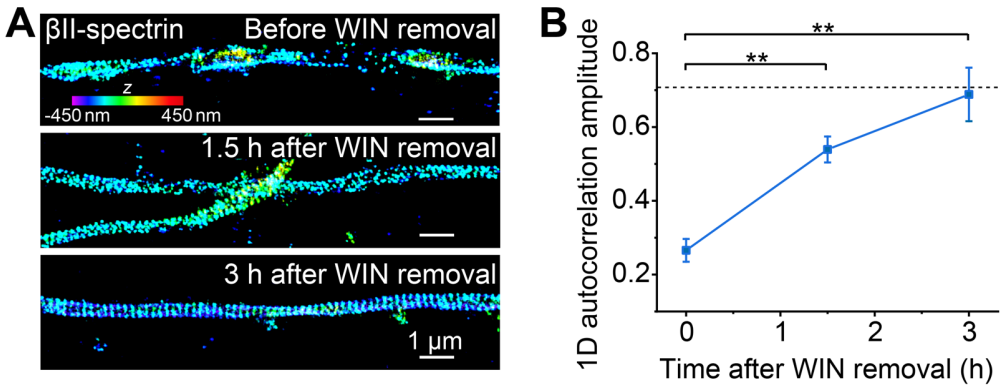

Fig. S17. Recovery of the MPS upon ligand removal. (A) 3D STORM images of βII-spectrin in CB1-positive axons of neurons treated with WIN for 1 hr, and of neurons recovered for 1.5 hr and 3 hr after WIN removal. The STORM image obtained immediately following 1-hr WIN treatment (top panel) is reproduced from Fig. 4A for comparison. Scale bars: 1 μm. Colored scale bar indicates the z-coordinate information. **(B)** Average 1D auto-correlation amplitude of the βII-spectrin distribution, indicating the degree of the periodicity in the MPS, calculated from many axon segments at different time points after WIN removal following 1-hr WIN treatment. The data point at time zero is reproduced from Fig. 4B for comparison, and the dashed line represents the average 1D auto-correlation amplitude of the βII-spectrin distribution before WIN treatment reproduced from Fig. 4B for reference. Data are mean ± s.e.m. (n = 3 biological replicates; 50-100 axonal regions were examined per condition).**: $P < 0.01$; actual P values (from left to right): 4.2×10^{-3}, 5.9×10^{-3} (unpaired Student's t test).

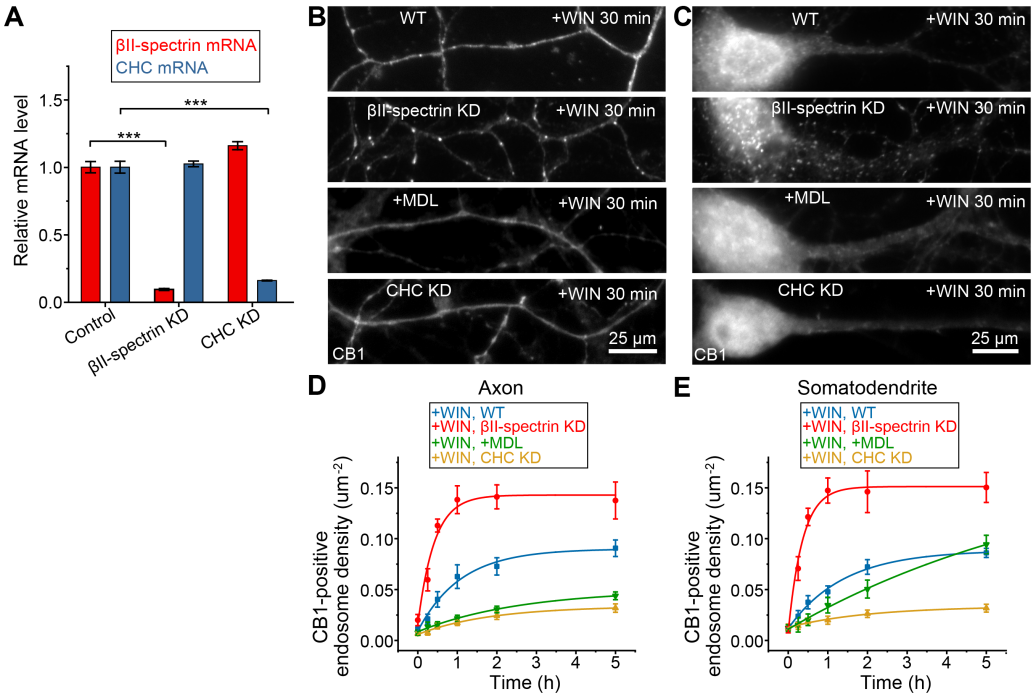

Fig. S18. Endocytosis of CB1 upon ligand binding in WT, βII-spectrin KD, MDL-treated, and clathrin heavy chain (CHC) KD neurons. (A) Quantitative RT-PCR results indicating the normalized mRNA expression levels of βII-spectrin (red) and CHC (blue) determined for neurons transfected with adenoviruses expressing scrambled (control) shRNA (left two bars), βII-spectrin shRNA (middle two bars), or CHC shRNA (right two bars). Data are mean ± s.e.m. ($n = 3$ biological replicates). ***: $P < 0.001$; actual P values (from left to right): 2.9×10^{-5}, 4.5×10^{-5} (unpaired Student's t test). The data in fig. S6A were reproduced here for comparison. **(B, C)** Fluorescence images of CB1 in the axons (B) and somatodendritic regions (C) of WT neurons, βII-spectrin KD neurons and CHC KD neurons treated with WIN for 30 min, as well as of WT neurons treated with WIN for 30 min in the presence of the calpain inhibitor MDL. Scale bars: 25 μm. **(D, E)** Time courses of CB1 endocytosis in axons (D) and somatodendritic regions (E) after WIN addition, quantified by the density of CB1 endosomes (i.e. CB1-positive fluorescence puncta). Solid lines represent single-exponential fits of the data. Blue: WT neurons; Red: βII-spectrin KD neurons; Green: WT neurons treated with MDL; Yellow: CHC KD neurons. Data are mean ± s.e.m. ($n = 3$ biological replicates).

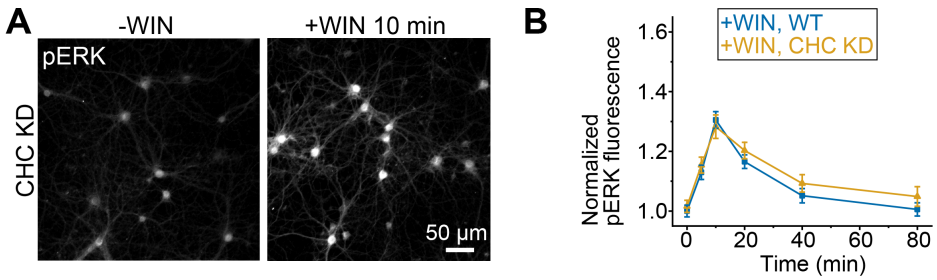

Fig. S19. Effect of endocytosis inhibition on WIN-induced ERK signaling. (A) Immunofluorescence images of pERK in CHC KD neurons before (left) and 10 min after (right) addition of the CB1 ligand WIN. Scale bars: 50 µm. **(B)** Time courses of ERK activation for WT (blue) and CHC KD (yellow) neurons after initiating the WIN treatment. The curve for WT neurons in (B) is reproduced from Fig. 2C. Data are mean ± s.e.m. (n = 3 biological replicates; 20-30 imaging regions were examined per condition).